LAWRENCE
LIVERMORE
NATIONAL
LABORATORY

UCRL-TR-234075

Hydra modeling of experiments to study ICF capsule fill hole dynamics using surrogate targets

James B. Elliott

August 28, 2007

This work was performed under the auspices of the U.S. Department of Energy by University of California, Lawrence Livermore National Laboratory under Contract W-7405-Eng-48.

Title

J. B. Elliott
Lawrence Livermore National Laboratory, Livermore, California, 94550
(Dated: August 3, 2007)

Abstracty

PACS numbers:

I. COMPUTATIONAL MODEL

In this section the results of HYDRA [1] design simulations will be discussed. The simulations were conducted in two dimensional, RZ geometry, with the fill tube on axis. The radiation transport was treated in the diffusion approximation using 15 energy groups. Opacities were calculated ... The equations of state (EOS) for all materials used were from a combined analytic / Thomas-Fermi EOS which uses a modified Cowan model for the ion EOS, and uses a scaled Thomas-Fermi table for the electron EOS.

A. Initial configuration

The initial setup of the computation model is shown, schematically, in Fig. 1. The physical dimensions of the model are 0.0 cm $\leq R \leq$ 0.025 cm and -0.1 cm $\leq Z \leq$ 0.6 cm.

From -0.1 cm $\leq Z \leq$ 0.0 cm is carbonized resorcinol formaldehyde (CRF) at an initial temperature of $T_0 = 10^{-6}$ KeV and an initial density of $\rho_0 = 0.05$ g/cm^3.

From 0.0 cm $\leq Z \leq$ 0.03 cm is copper doped beryllium (3% copper by atom) at an initial temperature of $T_0 = T_{\rm ph}$ (where the subscript is for "pre-heat" as will be discussed below) and initial density of $\rho_0 = 1.848$ g/cm^3.

A cylindrically symmetric cavity of dimension 0.0 cm $\leq R \leq$ 0.0025 cm by 0.0 cm $\leq Z \leq$ 0.02 cm in the copper doped beryllium is filled with helium at an initial temperature of $T_0 = 10^{-6}$ KeV and an initial density of $\rho_0 = 10^{-4}$ g/cm^3.

From 0.03 cm $\leq Z \leq$ 0.0308 cm is parylene-N at an initial temperature of $T_0 = 10^{-6}$ KeV and an initial density of $\rho_0 = 1.11$ g/cm^3. This serves as an ablator.

Finally, from 0.0308 cm $\leq Z \leq$ 0.6 cm is helium at an initial temperature of $T_0 = 10^{-6}$ KeV and an initial density of $\rho_0 = 1.25 \times 10^{-4}$ g/cm^3.

B. Temperature source

A Planckian temperature source is incident from $Z =$ 0.6 cm. The temperature of the source as a function of time is shown in Fig. 2. A Dante measurement (heavy solid curve) gives a temperature profile measured in the experiment. The initial 1 ns (approximate) of the Dante measurement was removed in the computational results given below. The inclusion of the first 1 ns (approximate) has no effect on the results other than to change the overall timing by 1 ns.

Using the full temperature source yielded results that showed the interface of the CRF and copper doped beryllium (or pedestal) moved faster than what was observed in experiment. The experiment shows that at a time of $t = 15$ ns the pedestal was 177 μm beyond it initial position or in terms of the computational model the pedestal was located at $Z = -177$ μm.

The source profile was scaled down and the location of the pedestal at $t = 15$ ns was recorded. Results are shown in Fig 3. The results were fit to a fourth order polynomial. That fit was used to find the best agreement of the pedestal location at $t = 15$ ns between the computational model and experiment. This procedure indicates that scaling the initial source by 88.5679% gives the best agreement.

C. General description of jet evolution

The following describes the behavior of the simulation with an initial temperature of the copper doped beyrllium of $T_{\rm ph} = 10^{-6}$ KeV. At the start of the simulation the temperature source is applied from the far right of the model. The parylene-N is heated and ablates, launching a flat shock wave through the copper doped beryllium, see Fig. 4.

The shock wave reaches the bottom of the cavity at a time of about $t = 2.6$ ns and pushes it forward. Refractions, reflections and the subsequent interference of the shock as it moves through the cavity gives rise to the shape of the jet. As a rough approximation the overall shape and size of the jet for times $t \leq 10$ ns is the inverse of the cavity.

Far from the cavity the shock progresses undisturbed by the presence of the cavity. The shock wave reaches the interface of the CRF and the copper doped beryllium at $t = 8.7$ ns. The shock traverses the copper doped beryllium in 6.1 ns, thus it travels at an average speed of approximately 49.18 μm/ns. The shock moves ahead of the CRF, copper doped beryllium interface (which is itself moving at an average speed of 28.25 μm/ns) and travels through the CRF at an average speed of 36.51 μm/ns.

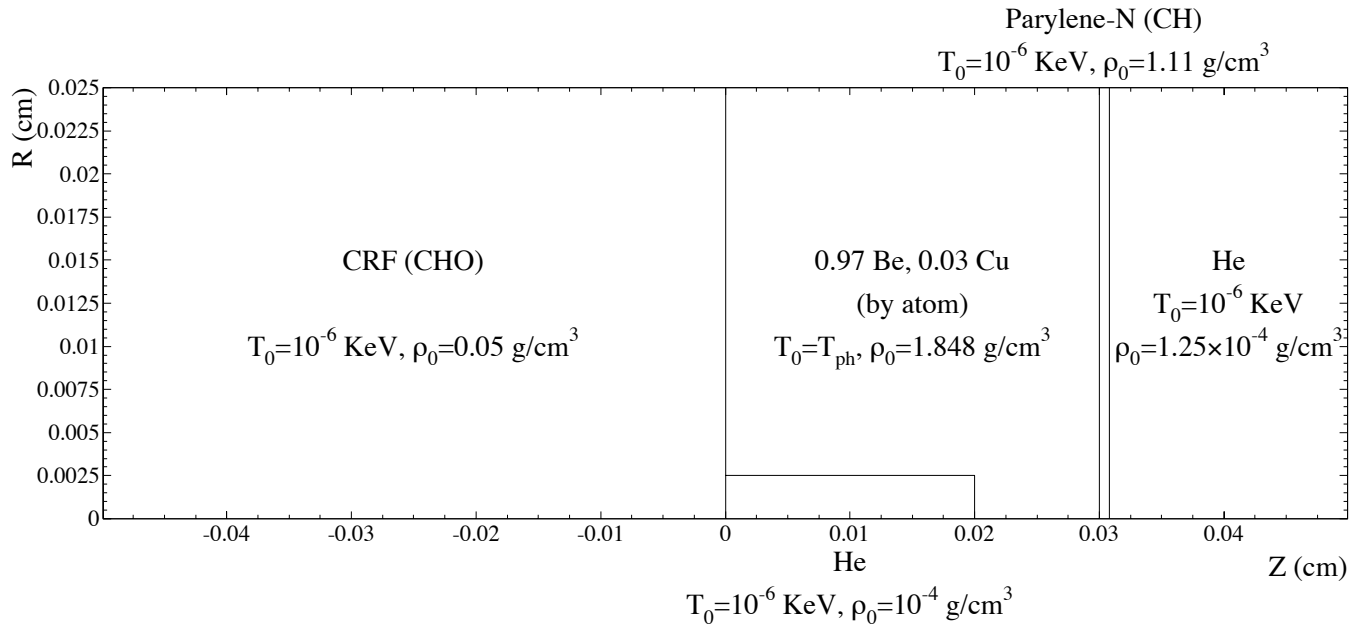

FIG. 1: A schematic of the initial configuration of the model, not to scale. See text for more detail. The temperature source is incident from the right.

D. Results

Three metrics from the experimental results were used to "grade" the results of the computational model. These metrics are the mass: of the jet, the height of the jet and the location of the shock wave ahead of the pedestal. The results from the simulations for these metrics at time $t \approx 15$ ns are shown in Figures 5, 6 and 7.

The first simulation performed used an initial temperature of the copper doped beryllium of $T_0 = T_{\rm ph} = 10^{-6}$ KeV. The results of that simulation gave a jet mass $M_{\rm jet}$ that was over twice the value of the experimental result (see the left most point on Fig. 5) and a jet height that was about 1.5 times the experimental result (see the left most point on Fig. 6).

The height of the pedestal observed in simulation agreed well with the experimental results, however this is to be expected since the temperature source was adjusted to match the experimentally determined location of the pedestal at the time $t = 15$ ns and the time at which the simulation was sampled (shown in Fig. 8) was chosen to maximize agreement of the height of the beryllium pedestal between simulation and experiment. The location of the shock ahead of the pedestal agrees well between experiment and simulation.

It was then observed that increasing the initial temperature $T_{\rm ph}$ of the copper doped beryllium lead to a lower jet mass, a smaller jet height with little effect on the location of the pedestal. A set of 14 simulations were performed systematically changing the initial temperature of the copper doped beryllium over a range of 10^{-6} KeV $\leq T_{\rm ph} \leq 10^{-3}$ KeV.

There is a large range of initial temperatures (2×10^{-4} KeV $\leq T_{\rm ph} \leq 10^{-3}$ KeV) that give values of the jet mass that are within the experimental error bars. However, only for $T_{\rm ph} \geq 8.0 \times 10^{-4}$ KeV are the results for the pedestal location within about five percent of the experimental results with the best agreement being at $T_{\rm ph} = 9.0 \times 10^{-4}$ KeV.

As mentioned above, the height of the beryllium pedestal observed in simulations agrees with the experimental results because the temperature source was chosen to insure that agreement and also because the time at which the simulation was sampled was chosen maximize agreement of the height of the beryllium pedestal between simulation and experiment. The height of the shock ahead of the beryllium pedestal observed in the simulation agrees with the experimental results to within ten percent for all values of $T_{\rm ph}$.

1. *Copper doped beryllium "pre-heat"*

Physically, the initial temperature of the copper doped beryllium $T_{\rm ph}$ may be due to "pre-heating" of the substance arising from fast, deeply penetrating radiation. The melting temperature of beryllium is 1.34×10^{-4} KeV and the melting point of copper is 1.17×10^{-4} KeV.

When the copper doped beryllium is pre-heated and melts, it flows into the cavity thereby closing it. Figures 9 and 10 show how much copper doped beryllium is pre-heated has flowed into the hole and the radius of the hole at the time at which the shock due to the temperature

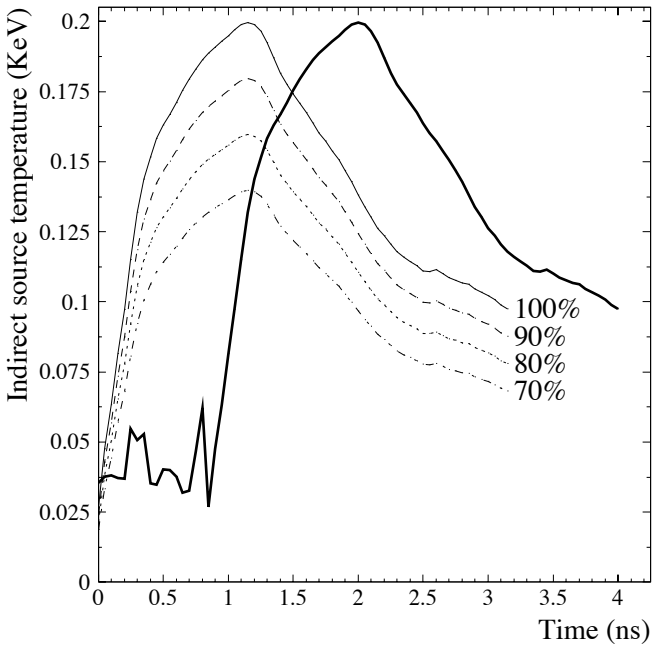

FIG. 2: The temperature (in KeV) as a function of time (in ns) for the input temperature source used in the computations. The heavy solid curve shows the source profile given by a Dante measurement. The lighter curves shows the temperature profile with the initial 1 ns (approximate) removed and then scaled.

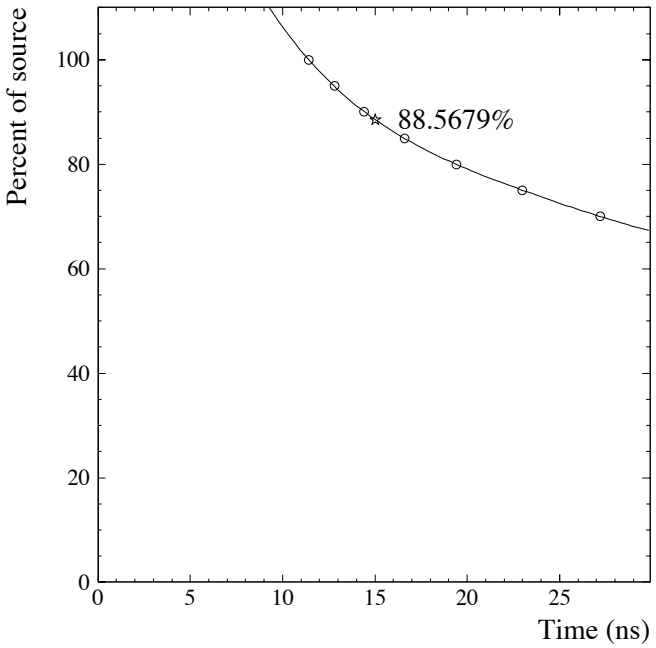

FIG. 3: The percent by which the temperature source was scaled as a function of the time of pedestal matching. Open circles show the results of computations. The solid line is a fit of a fourth order polynomial to the open circles. The open star shows percent by which the temperature source should be scaled to obtain the best pedestal matching.

source arrives at the bottom of the cavity. The greater the pre-heat temperature, the smaller the cavity through which the shock due to the temperature source travels and, in general, the less massive and spatially smaller the jet.

2. The $M_{\rm jet}$ shoulder

Generally, Fig. 5 shows the mass of the beryllium jet decreasing as initial temperature of the copper doped beryllium increases. However, there is a "shoulder" in this trend that starts at $T_{\rm ph} = 3 \times 10^{-4}$ KeV and ends at $T_{\rm ph} = 6.0 \times 10^{-4}$ KeV. This shoulder is an artifact of the method used to determine the mass of the jet.

Figure 11 shows four simulations which give rise to the $M_{\rm jet}$ shoulder. The algorithm used to define the jet is: all copper doped beryllium beyond the pedestal, or above the cut off boundary, is part of the jet (see horizontal dashed lines in Fig. 11). As the initial temperature of the copper doped beryllium is increased, the base of the jet (the region of highest beryllium density) widens. Also as the initial temperature of the copper doped beryllium is increased, the pedestal becomes less smooth (see the sections circled in Fig. 11). These two effects compete. As the base of the jet widens, the mass of the jet increases. As the pedestal smoothness decreases, the cut off boundary of the jet rises and the mass of the jet decreases. Eventually, the decrease in pedestal smoothness effect dominates and the trend of decreasing jet mass is resumed.

The overall trend of decreasing jet mass with increasing initial temperature of the copper doped beryllium is a real and physical effect as will be discussed below.

3. The jet height peak

As with the mass of the jet, the general trend is that the height of the decreases as the initial temperature of the copper doped beryllium increases. However, Fig. 6 shows that there is a "peak" in the jet height with a maxium at $T_{\rm ph} = 6 \times 10^{-4}$ KeV. Figure **??** shows the change in the shape and height of the jet as a function of $T_{\rm ph}$.

The contraction of the cavity gives rise to supersonic pressure waves which propagate through the helium. This interaction of the shock due to the temperature source and the pressure wave in the cavity due to the flow of the copper doped beryllium into the cavity greatly affects the spatial size and shape of the jet. The speed of the pressure waves in the cavity depend on the speed with which the copper doped beryllium flows into the cavity, which in turn depends on it's initial temperature. For lower values of $T_{\rm ph}$ the pressure wave in the cavity does not travel far by the time the shock due to the tem-

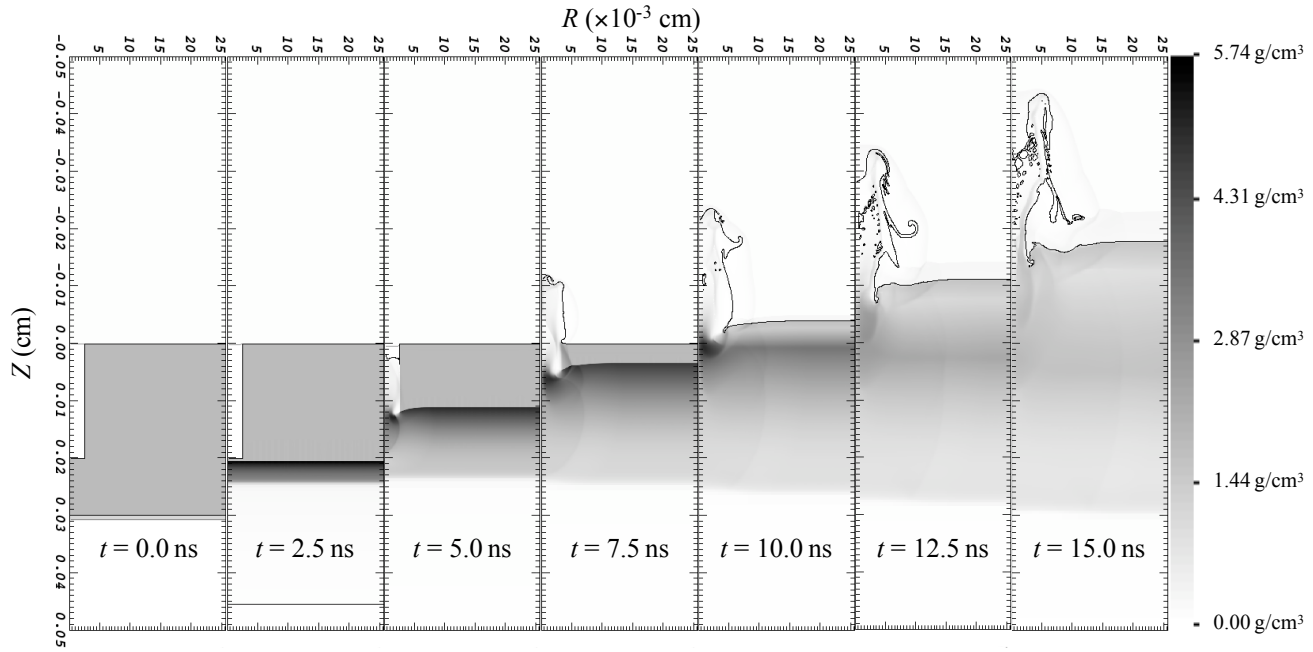

FIG. 4: The simulation with an initial temperature of the copper doped beyrllium of $T_{\rm ph} = 10^{-6}$ KeV at various times. The gray scale shows the density of the materials. The solid line shows the interface between the CRF (top) and the copper doped beryllium (bottom).

perature source completes its transit through the cavity. For higher values of $T_{\rm ph}$ the pressure wave in the cavity travels to the axis of symmetry ($R = 0.0$ cm) by the time the shock due to the temperature source completes its transit through the cavity. For even higher values of $T_{\rm ph}$ the pressure wave in the cavity has been reflected at the axis of symmetry ($R = 0.0$ cm) and is traveling back towards the wall of the cavity by the time the shock due to the temperature source completes its transit through the cavity.

For initial temperatures $T_{\rm ph} \leq 4 \times 10^{-4}$ KeV the pressure waves are slow and weak and have little interaction with the shock due to the temperature source and the spatial size of the jet decreases because the cavity size decreases.

For larger initial temperatures 5×10^{-4} KeV $\leq T_{\rm ph} \leq 6 \times 10^{-4}$ KeV pressure wave velocities are less than zero (i.e. moving towards $R = 0.0$ cm) and interact with the shock from the temperature source to cause spatially larger jets. At $T_{\rm ph} = 6 \times 10^{-4}$ KeV the pressure wave just reaches the axis of the cavity when the shock wave due to the temperature source reaches the top of the cavity and the jet reaches it's maximum spatial extent.

For $T_{\rm ph} > 6 \times 10^{-4}$ KeV the pressure wave in the cavity has reached the axis, been reflected and is traveling back towards the wall of the cavity when the shock wave due to the temperature source reaches the top of the cavity and the spatial extent of the jet begins to decrease.

The pressure wave in the cavity acts to forward focus the jet. When the pressure wave is far from the axis during the shock transit through the cavity (i.e. for $T_{\rm ph} < 6 \times 10^{-4}$ KeV) or when the pressure wave has been reflected (i.e. for $T_{\rm ph} > 6 \times 10^{-4}$ KeV) the forward focusing is less than when the pressure wave is closest to the axis (i.e. when $T_{\rm ph} = 6 \times 10^{-4}$ KeV).

E. Jet Suppression

As demonstrated above, some pre-heating of the copper doped beryllium closes the cavity which, in general, leads to less massive and spatially smaller jets. If the shock is delayed until the cavity is nearly filled there is almost complete suppression of the jet and a uniform shock front is observed. This is shown in Fig. 12 where the copper doped beryllium was pre-heated to a temperature of $T_{\rm ph} = 9 \times 10^{-4}$ KeV and the temperature source was delayed by 2.1 ns.

Simulations with material of higher density filling the cavity in the copper doped beryllium show similar results. Specifically, at about 13 ns after application of the temperature source, simulations of a pre-heated copper doped beryllium and delayed temperature source yielded a 94% reduction in the mass of the jet as compared to a zero pre-heat, no delay simulation.

There may be additional benefits to pre-heating, namely any surface roughness would be smoothed out by the surface tension of the now liquid copper doped beryllium. This would occur in a fashion similar to the closing of the cavity demonstrated above. Unfortunately, HYDRA is not able to easily simulate the effects of surface tension. Also any crystalline in the copper doped

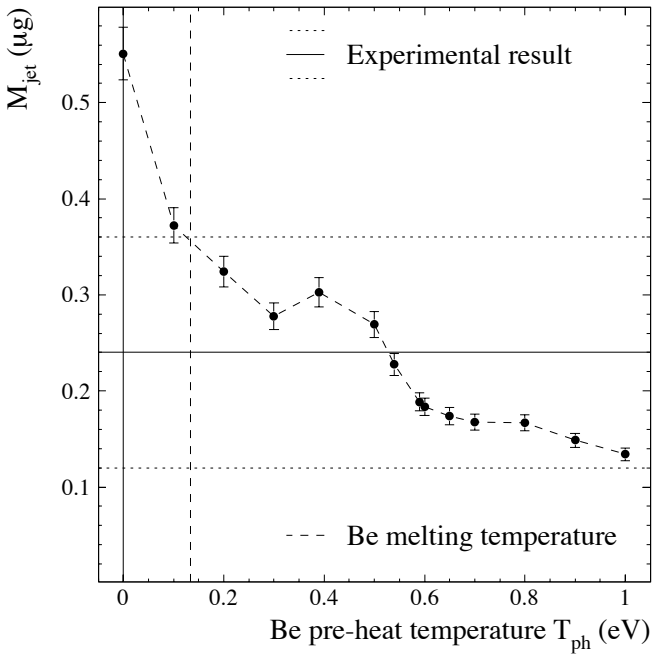

FIG. 5: The mass of the beryllium jet $M_{\rm jet}$ as a function of beryllium pre-heat temperature $T_{\rm ph}$ in KeV at time t ns. Error bars are estimated to be ten percent of the value of $M_{\rm jet}$. A dashed line connects the results to guide the eye. The horizontal solid (dotted) line(s) shows the mean (errors on the) experimental results. The vertical dashed line shows the melting temperature of beryllium. Note the "shoulder" for 3×10^{-4} KeV $\leq T_{\rm ph} \leq 6 \times 10^{-4}$ KeV. The shoulder is an artifact arising from the method used to determine $M_{\rm jet}$. See text for details.

beryllium would vanish, leaving a more uniform medium through which any shock waves would travel.

[1] M. M. Marinak *et al.*, Phys. Plasmas **8**, 2275 (2001).

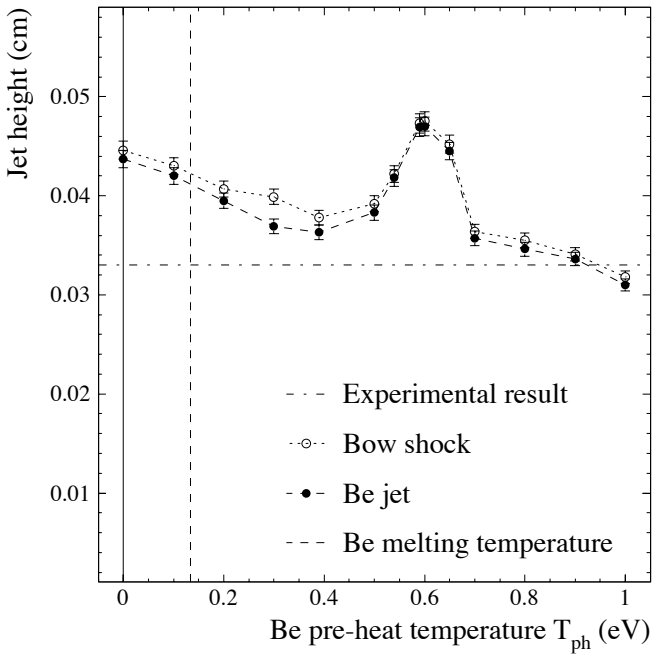

FIG. 6: The height of the jet in cm as a function of beryllium pre-heat temperature $T_{\rm ph}$ in KeV at time $t \approx 15$ ns. Open circles show the height of the bow shock, dotted lines join the data points to guide the eye. Closed circles show the height of the beryllium jet, dashed lines join the data points to guide the eye. The horizontal dash-dotted line shows the experimental result. The vertical dashed line shows the melting temperature of beryllium.

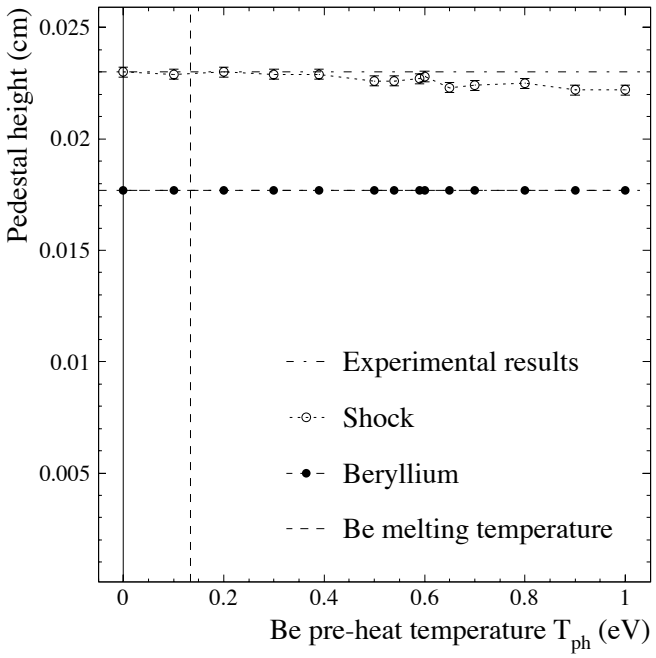

FIG. 7: The height of the pedestal in cm as a function of beryllium pre-heat temperature $T_{\rm ph}$ in KeV at time $t \approx 15$ ns. Open circles show the height of the shock, dotted lines join the data points to guide the eye. Closed circles show the height of the beryllium pedestal, dashed lines join the data points to guide the eye. The horizontal dash-dotted lines show the experimental results. The vertical dashed line shows the melting temperature of beryllium.

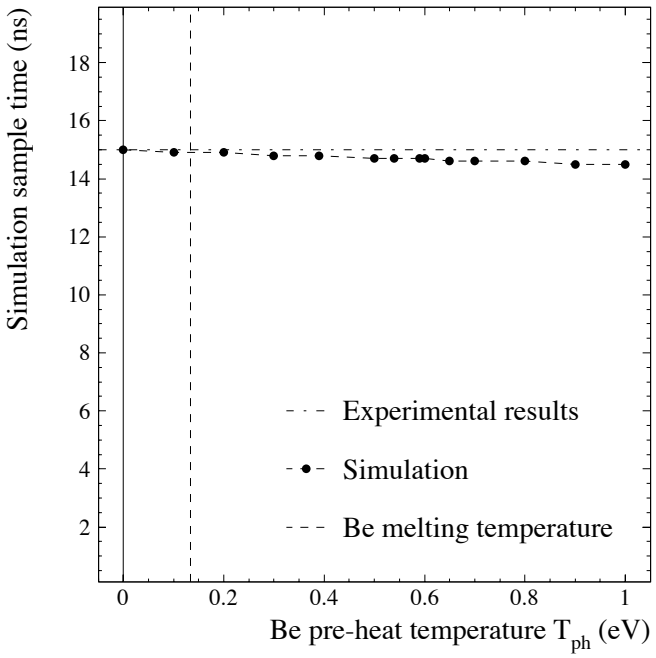

FIG. 8: The time (in ns) at which the simulation was sampled as a function of beryllium pre-heat temperature $T_{\rm ph}$ in KeV. Dashed lines join the data points to guide the eye. The horizontal dash-dotted lines show the time at which the experimental results were measured: $t = 15$ ns. The vertical dashed line shows the melting temperature of beryllium.

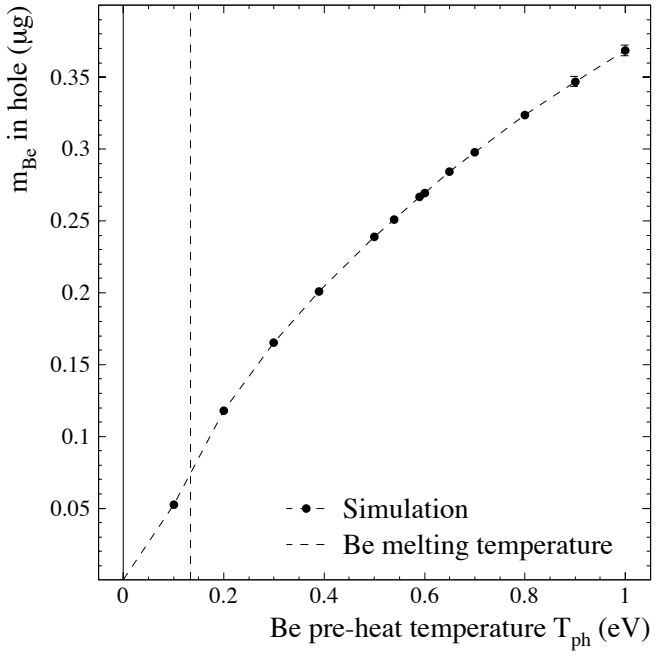

FIG. 9: The mass of copper doped beryllium $m_{\rm Be}$ that has flowed into the cavity as a function of the initial temperature of the copper doped beryllium $T_{\rm ph}$ at the time when the shock due to the temperature source arrives at the bottom of the cavity. Dashed lines connect the data points to guide the eye. The vertical dashed line shows the melting temperature of beryllium.

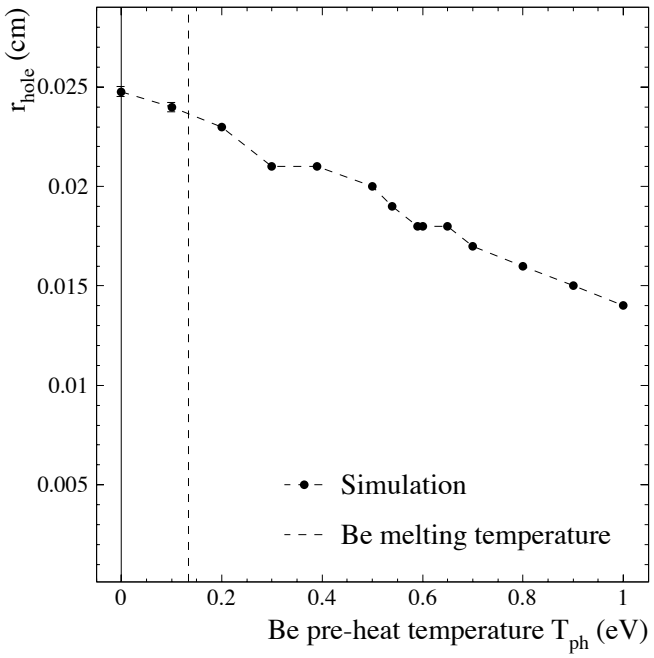

FIG. 10: The radius of the cavity $r_{\rm cavity}$ as a function of the initial temperature of the copper doped beryllium $T_{\rm ph}$ at the time when the shock due to the temperature source arrives at the bottom of the cavity. Dashed lines connect the data points to guide the eye. The vertical dashed line shows the melting temperature of beryllium.

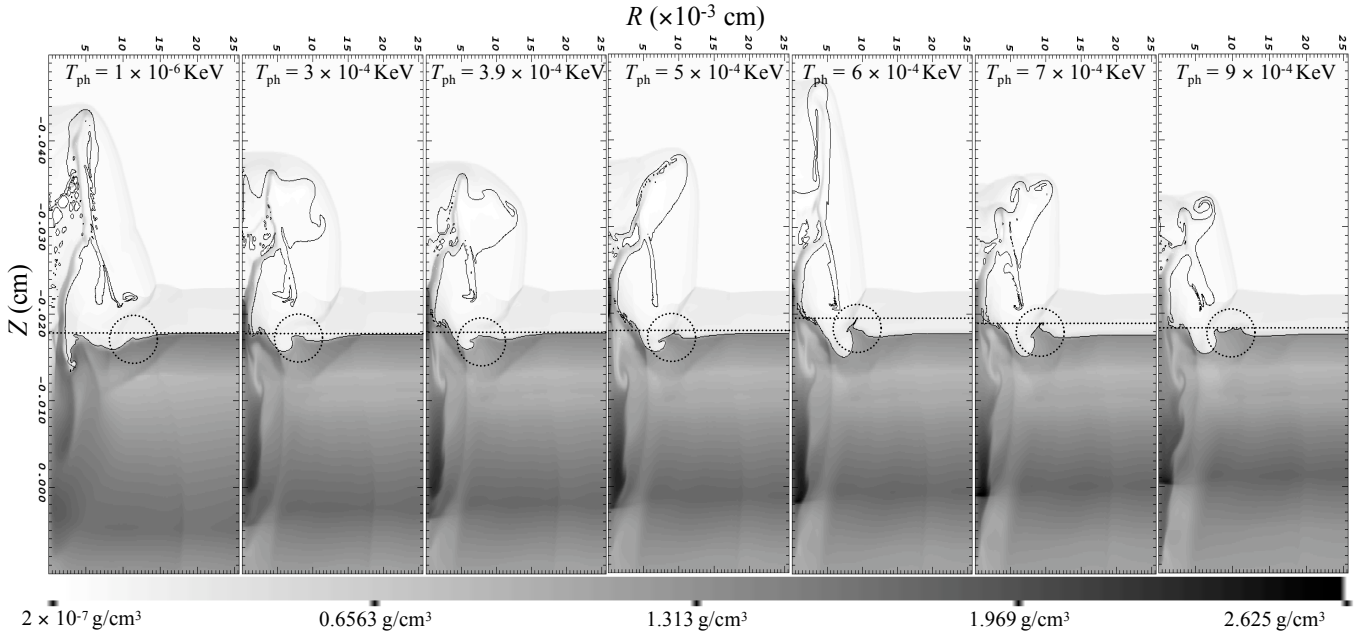

FIG. 11: The beryllium jet at time $t \approx 15$ns for the simulations which give rise to the "shoulder" shown in Fig. 5. The gray scale shows the density of the materials. The solid line shows the interface between the CRF (top) and the copper doped beryllium (bottom). The dashed line shows the cut off boundary which defines the jet: any copper doped beryllium above the dashed line is considered part of the jet. The circles highlight a portion of the pedestal that changes the position of the cut off boundary. See text for further discussion. Also evident is the "peak" in jet height shown in Fig. 6. As the initial temperature of the copper doped beryllium is increases the height of the jet increases until $T_{\rm ph} = 6 \times 10^{-4}$ KeV, thereafter the height of the jet decreases with increasing initial temperature of the copper doped beryllium. See text for further discussion.

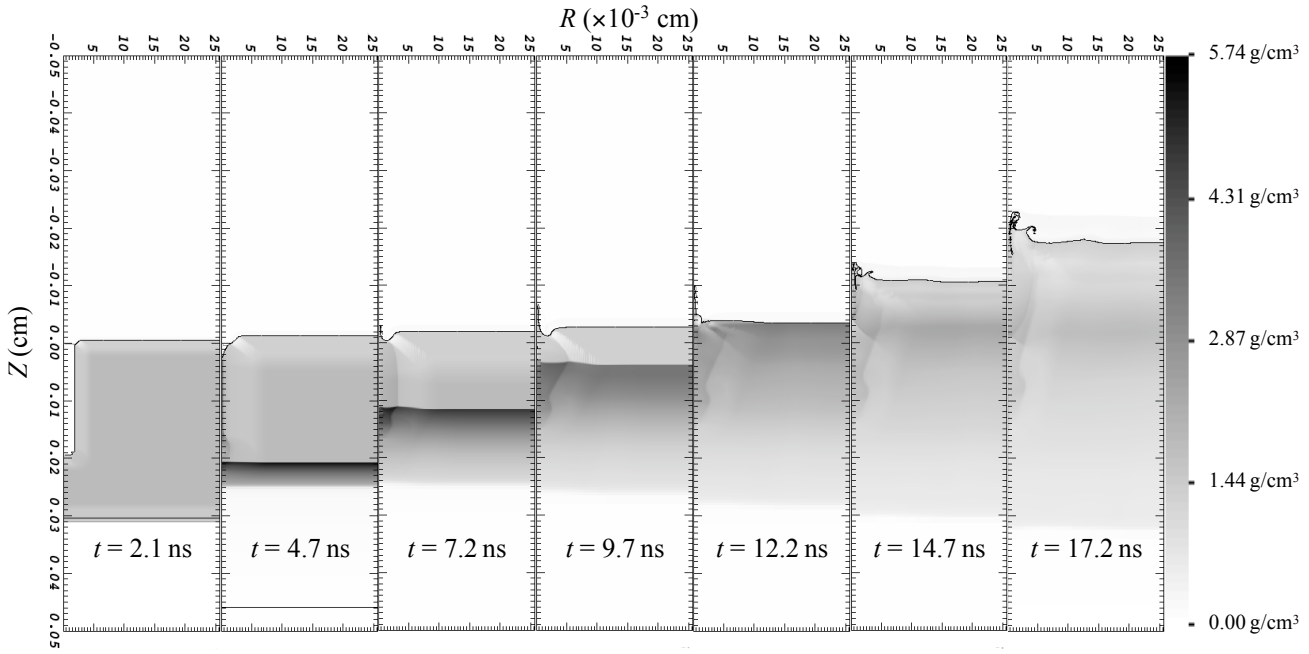

FIG. 12: The simulation with an initial temperature of the copper doped beyrllium of $T_{\rm ph} = 9 \times 10^{-6}$ KeV at various times. The gray scale shows the density of the materials. The solid line shows the interface between the CRF (top) and the copper doped beryllium (bottom). A uniform shock is produced by pre-heating the copper doped beryllium to a temperature of $T_{\rm ph} = 9 \times 10^{-4}$ KeV and delaying the temperature source by 2.1 ns. At late times there is still a beryllium jet, but it's height is less than the height of the shock wave ahead of the pedestal.